NASA TECHNICAL NOTE

NASA TN D-2062

N64 10183

NASA TN D-2062

A WIND-TUNNEL INVESTIGATION OF THE EFFECT OF CHANGES IN BASE CONTOUR ON THE DAMPING IN PITCH OF A BLUNTED CONE

by William R. Wehrend, Jr.

Ames Research Center
Moffett Field, California

NATIONAL AERONAUTICS AND SPACE ADMINISTRATION • WASHINGTON, D. C. • NOVEMBER 1963

258

TECHNICAL NOTE D-2062

A WIND-TUNNEL INVESTIGATION OF THE EFFECT OF CHANGES IN BASE CONTOUR ON THE DAMPING IN PITCH OF A BLUNTED CONE

By William R. Wehrend, Jr.

Ames Research Center
Moffett Field, California

NATIONAL AERONAUTICS AND SPACE ADMINISTRATION

NATIONAL AERONAUTICS AND SPACE ADMINISTRATION

TECHNICAL NOTE D-2062

A WIND-TUNNEL INVESTIGATION OF THE EFFECT OF CHANGES IN BASE CONTOUR ON THE DAMPING IN PITCH OF A BLUNTED CONE

By William R. Wehrend, Jr.

SUMMARY

The effects of a spherical segment afterbody on the damping in pitch of a blunted 12-1/2° cone were studied. Variations were made in the base radius, and the surface of the shortest radius base was modified by annular steps, both in and out, and by annular fences. The Mach number range for the test was 0.25 to 2.20, and the angle-of-attack range from -4° to +18°.

The results of the tests showed that decreasing the radius of the spherical base caused an unstable shift in the damping moment. This change was large enough to cause unstable damping in the subsonic speed range. The surface modifications to the base did have some corrective effect on the damping, but not sufficient to stabilize the model at subsonic speeds.

INTRODUCTION

Reports of several investigations, such as reference 1, have shown that blunted cones with flat bases are statically stable in both forward and rearward flight. Although the angle range for static stability in rearward flight is considerably smaller than for forward flight, the possibility remains that a vehicle having these characteristics and no active control system could remain in either attitude. It would probably not be practical to provide heat protection for both flight attitudes and, therefore, the vehicle must be designed so that it is stable in only one position. The stability in the rearward attitude can be eliminated by the addition of an appropriate spherical or conical fairing on the base of the vehicle (ref. 1), but such fairings may bring on a dynamic stability problem. It is shown in reference 2 that a spherical segment base fairing caused a reduction in the level of the damping-in-pitch moment, and this reduction was large enough that in the subsonic speed range it might cause dynamic instability. The present investigation was undertaken to provide additional information on the effects of base modifications on the damping in pitch.

Experiments were conducted in the Ames 6- by 6-Foot Supersonic Wind Tunnel with the basic blunted cone of reference 2. The model was a 12-1/2° semivertex angle cone with a spherically blunted tip. Damping-in-pitch moments and static stability were measured with various base modifications in the Mach number range from 0.25 to 2.20, and angles of attack from -4° to +18°. The modifications included several spherical segment bases, annular fences normal to a spherical base, and discontinuities in the spherical base. These modifications were intended to retain the rearward flight static instability characteristics of cones with spherical bases while causing a minimum disturbance to the forward flight characteristics.

SYMBOLS

C_A axial-force coefficient, $\frac{\text{axial force}}{(1/2)\rho V^2 S}$

C_{D_o} drag coefficient, at zero angle of attack, $\frac{\text{drag force}}{(1/2)\rho V^2 S}$

C_L lift coefficient, $\frac{\text{lift force}}{(1/2)\rho V^2 S}$

C_m pitching-moment coefficient, $\frac{\text{pitching moment}}{(1/2)\rho V^2 SD}$

$C_{m_q} + C_{m_{\dot{\alpha}}}$ damping-in-pitch coefficient, $\frac{\partial C_m}{\partial\left(\frac{qd}{V}\right)} + \frac{\partial C_m}{\partial\left(\frac{\dot{\alpha}d}{V}\right)}$, per radian

C_{m_α} pitching-moment curve slope at zero angle of attack, $\frac{\partial C_m}{\partial \alpha}$, per radian

C_N normal-force coefficient, $\frac{\text{normal force}}{(1/2)\rho V^2 S}$

C_{N_α} normal-force curve slope at zero angle of attack, $\frac{C_N}{\partial \alpha}$, per radian

D body base diameter

l body length

L distance along base surface

M Mach number

q pitching velocity

R	Reynolds number based on D
S	base area, $\frac{\pi D^2}{4}$
t	time
V	free-stream velocity
α	angle of attack, deg
$\dot{\alpha}$	variation of angle of attack with time, $\frac{d\alpha}{dt}$, radians/sec
ρ	air density

APPARATUS

Wind Tunnel and Balances

The tests were conducted in the Ames 6- by 6-Foot Supersonic Wind Tunnel which has a slotted floor and ceiling to permit testing at transonic Mach numbers. The Mach number range for the wind tunnel is 0.25 to 2.20.

The static forces and moments were measured on a conventional sting-mounted strain-gage balance. The sting used for the tests was 2 inches in diameter, and 23-1/2 inches long measured from the cone base. A photograph of a typical model installation is shown in figure 1.

The aerodynamic damping moments were measured with a single-degree-of-freedom forced-oscillation system which permits a small amplitude of oscillation (about $\pm 3\text{-}1/2^\circ$). A similar balance system is shown in reference 3. The balance on which the model was mounted is essentially a set of crossed flexures which act as a mechanical spring and also fix the oscillation axis of the model. The model is driven by an electromagnetic shaker in a pitching motion, and oscillates at some predetermined amplitude and at the natural frequency of the system. Measurements necessary for computing the damping moment were obtained from a calibrated strain-gage system within the balance. The models were sting mounted as shown in figure 1.

Models

The configuration chosen for the investigation was a blunted right circular cone with several variations in base contour. The semivertex angle of the conical section was $12\text{-}1/2^\circ$. The tip of the cone was a spherical segment with a ratio of tip radius to base diameter of 0.3. The base modifications were a series of spherical segments of different radius.

For convenience of comparing data, the model with the shortest base radius has been called the basic configuration. Dimensional details of this model are

shown on figure 2(a). The variations in base radius and the location of the center of curvature for each base are shown on figure 2(b). The modified spherical segment bases were all variations of the basic configuration, and take the form of either a step in the surface of the base or a sheet-metal fence mounted perpendicular to the base surface. These configurations are shown on figure 2(c).

The maximum diameter of the model was 6.36 inches. This diameter gives a ratio of model maximum diameter to wind-tunnel cross-section area of 0.00614.

TESTS AND PROCEDURES

The tests were conducted over a Mach number range from 0.25 to 2.20 and angles of attack from -4° to $+18^{\circ}$. The Reynolds number variation is shown on figure 3.

The quantities measured during the static portion of the test were normal force, axial force, and pitching moment. These various readings were reduced to coefficient form for presentation. The axial-force coefficient presented is the total axial force acting on the strain-gage balance with no adjustment of base pressure.

The quantity measured during the oscillation tests was the aerodynamic damping moment from which the parameter $C_{m_q} + C_{m_{\dot{\alpha}}}$ was evaluated. The damping moments were measured with the model oscillating $\pm 1\text{-}1/2^{\circ}$ about a nominal angle of attack.

The moment center used for the reduction of all the moment data is shown on figure 2(a), 0.562 D from the model base. The reference area and length were the maximum cross-section area of the model and the maximum diameter, respectively.

ACCURACY

Comparison of repeat points gives the following estimate of the accuracy of the data.

Static		Dynamic	
C_N	± 0.004	$C_{m_q} + C_{m_{\dot{\alpha}}}$	± 0.10
C_A	± 0.010		
C_m	± 0.001		
α	± 0.10		

RESULTS AND DISCUSSION

The measured variations of the static force and moment coefficients with angle of attack for the model with the short base radius are shown in figure 4. This model has been designated the basic configuration and has been used for comparison with other configurations. Only the data for the basic configuration have been shown on figure 4 because the base modifications had no measurable effect on the forward flight static characteristics.

The measured damping-moment coefficients are shown on figure 5 as a function of angle of attack for all configurations. Figures 5(a), 5(b), and 5(c) contain the damping coefficients for the model with the various base radii; figures 5(d), 5(e), and 5(f), for the models with the flat and stepped bases; and figures 5(g) and 5(h), for the models with the fences.

The static characteristics of figure 4 are summarized in figure 6 as a function of Mach number for an angle of attack of 0°. Note that the data of figure 4 are nearly linear and that the data of figure 6 are applicable over a moderate range of angles of attack.

The damping-moment coefficients for the model with the various bases are summarized as a function of Mach number in figures 7 and 8 for angles of attack of 0° and 15°, respectively. The upper curves show the effects of the various base radii; the middle curves, the effects of the steps in the base; and the lower curves, the effects of the fence.

As can be seen from figure 7, the only configuration that was dynamically stable at an angle of attack of 0° throughout the Mach number range was the model with the flat base.[1] All models with spherical-segment bases had a region of unstable damping in the subsonic speed range. The results show that as the base radius decreased, the damping moment became more unstable. Both the step-in and the step-out bases caused some shift of the damping moment in the stable direction at subsonic speeds, but produced a decrease in the damping moment in the higher Mach number range. This decrease in damping was small in the supersonic speed range for both steps, and also small for the step-in base in the transonic range. For the step-out base, the decrease in damping was fairly large in the transonic region. The greatest improvement at subsonic speeds was obtained with the step-in base.

The effect of the fences was a stable shift in the damping moment throughout most of the Mach number range. The regions of greatest change were at the high end of the supersonic region and at subsonic speeds. The change in damping in the transonic range was small. The improvement of the damping in the subsonic range was significant, but was not sufficient to correct the unstable characteristics. Perhaps a slightly higher fence might be able to completely eliminate the unstable region.

---

[1] A brief investigation of the influence of the model support and the internal configuration of the model on the damping moments is reported in reference 2. It is concluded from those results that for the purposes of the present report, the influence of these factors is not significant.

The unstable damping moment at subsonic speeds for the model with the spherical bases appears to be limited to angles of attack less than 15°. Although there is more scatter in the data at high angles of attack, figure 8 shows that the model had stable or neutrally stable damping at an angle of attack of 15° throughout the Mach number range with any of the base arrangements tested. The differences in damping at this angle of attack for the model with the various base modifications were small except in the transonic speed range.

CONCLUDING REMARKS

Wind-tunnel experiments have shown that a spherical-segment base affixed to a blunted shallow cone to produce rearward-flight static instability introduced unstable damping moments at subsonic speeds in forward flight. Increasing base radius and base modifications in the form of annular steps and fences on the base reduced the unstable damping moments, but failed to eliminate them. The unstable damping moments were limited to angles of attack less than 15° for all configurations.

Ames Research Center
National Aeronautics and Space Administration
Moffett Field, Calif., July 19, 1963

REFERENCES

1. Peterson, Victor L.: Motions of a Short 10° Blunted Cone Entering a Martian Atmosphere at Arbitrary Angles of Attack and Arbitrary Pitching Rates. NASA TN D-1326, 1962.

2. Wehrend, William R., Jr.: An Experimental Evaluation of Aerodynamic Damping Moments of Cones With Different Centers of Rotation. NASA TN D-1768, 1963.

3. Beam, Benjamin H.: A Wind-Tunnel Test Technique for Measuring the Dynamic Rotary Stability Derivatives at Subsonic and Supersonic Speeds. NACA Rep. 1258, 1956.

A-30160

Figure 1.- Photograph of model.

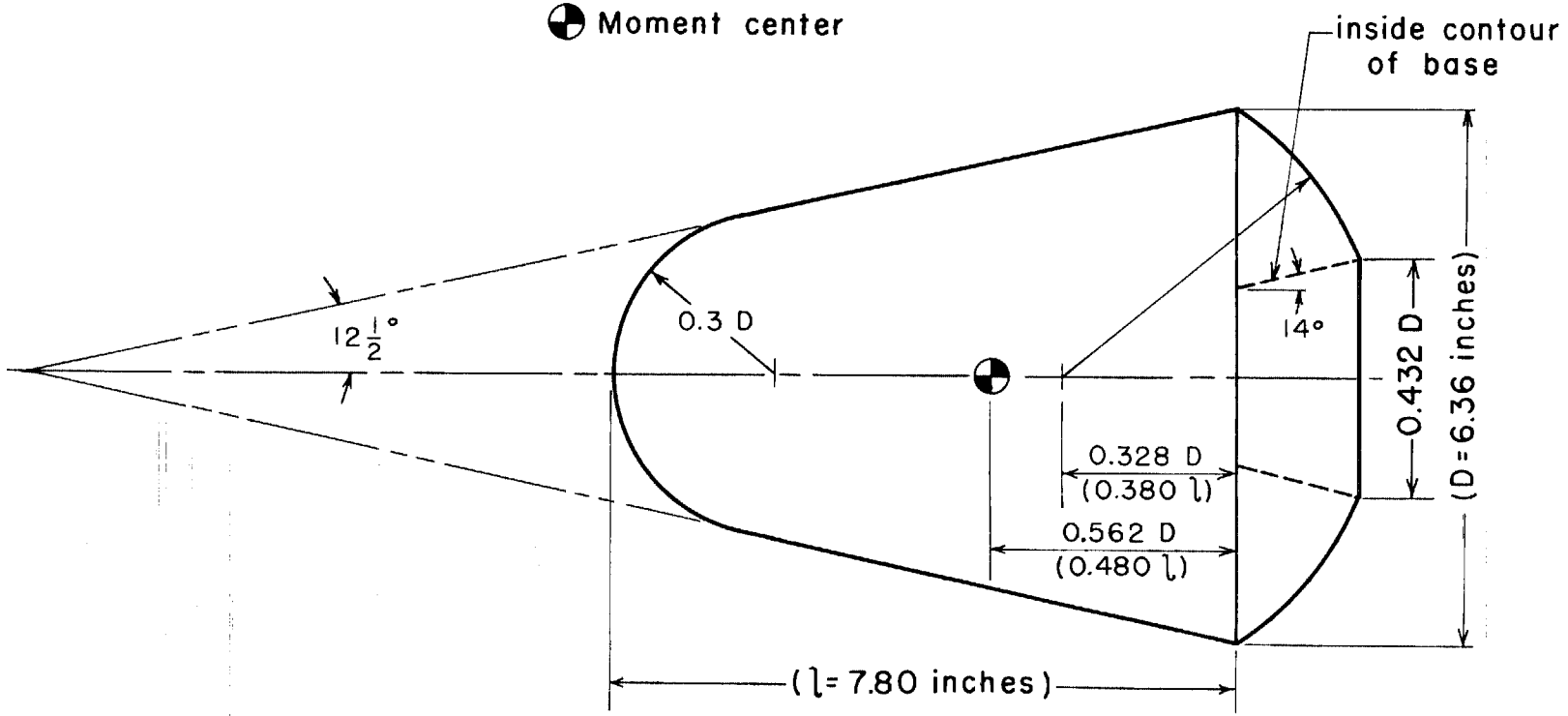

(a) Basic configuration

Figure 2.- Sketches of models.

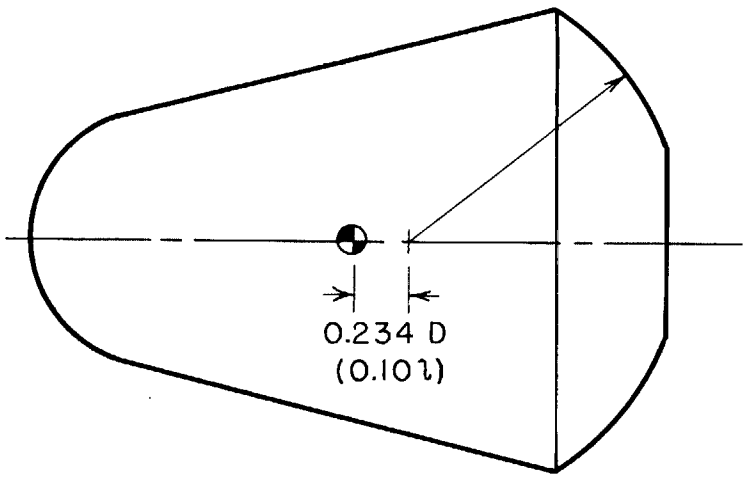

(a) Short base radius
(Basic configuration)

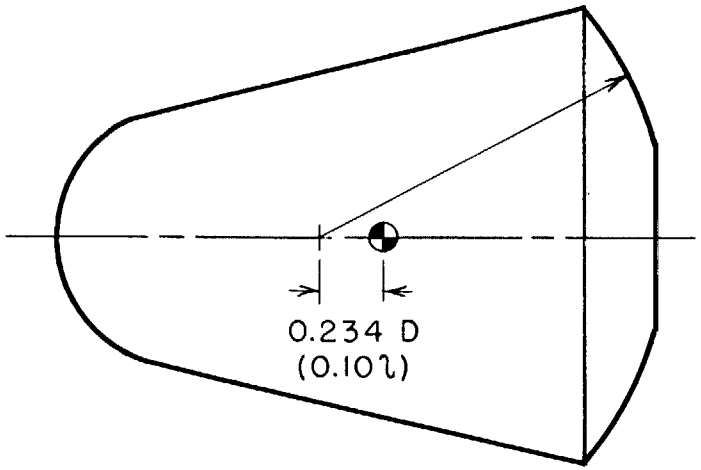

(c) Long base radius

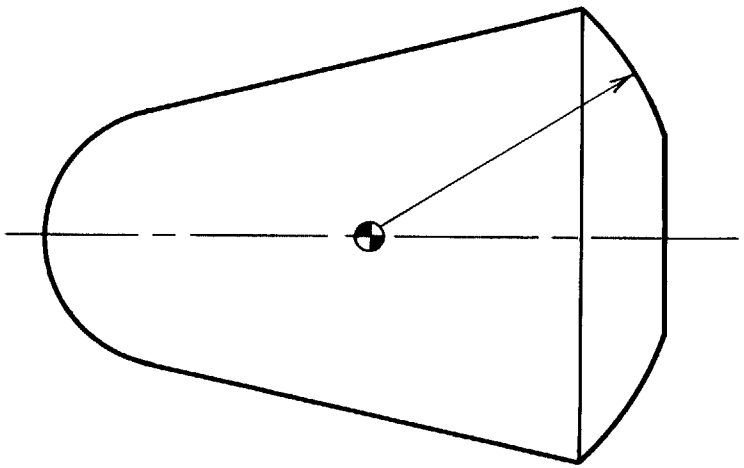

(b) Medium base radius

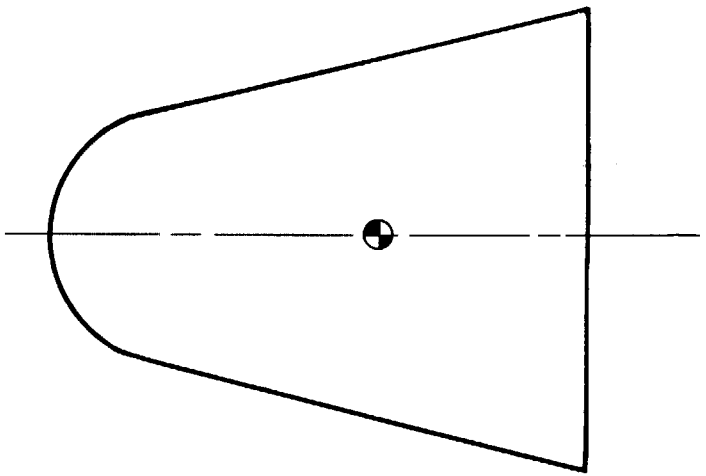

(d) Flat base

(b) Variation of base radius

Figure 2.- Continued.

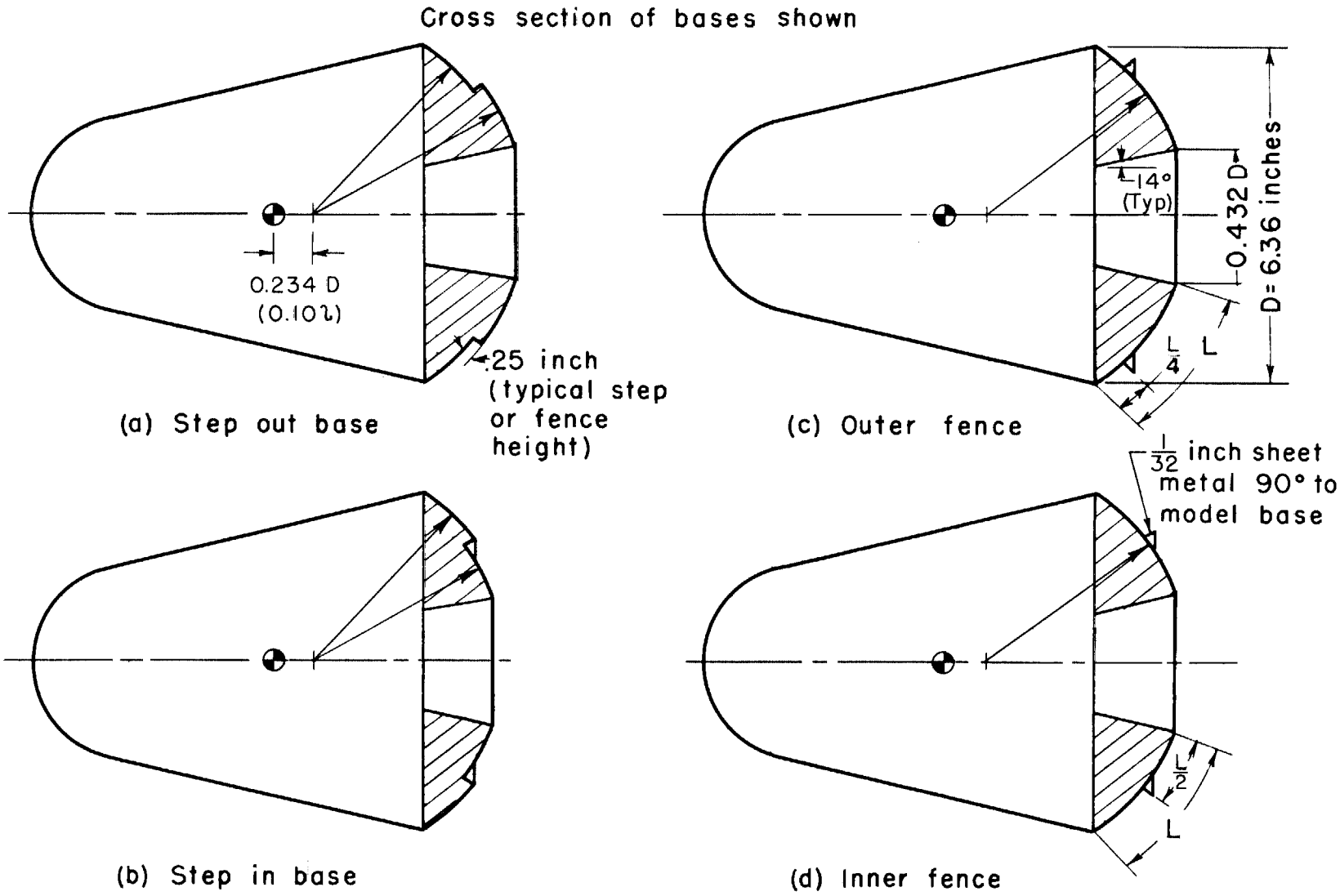

(c) Bases with steps and fences

Figure 2.- Concluded.

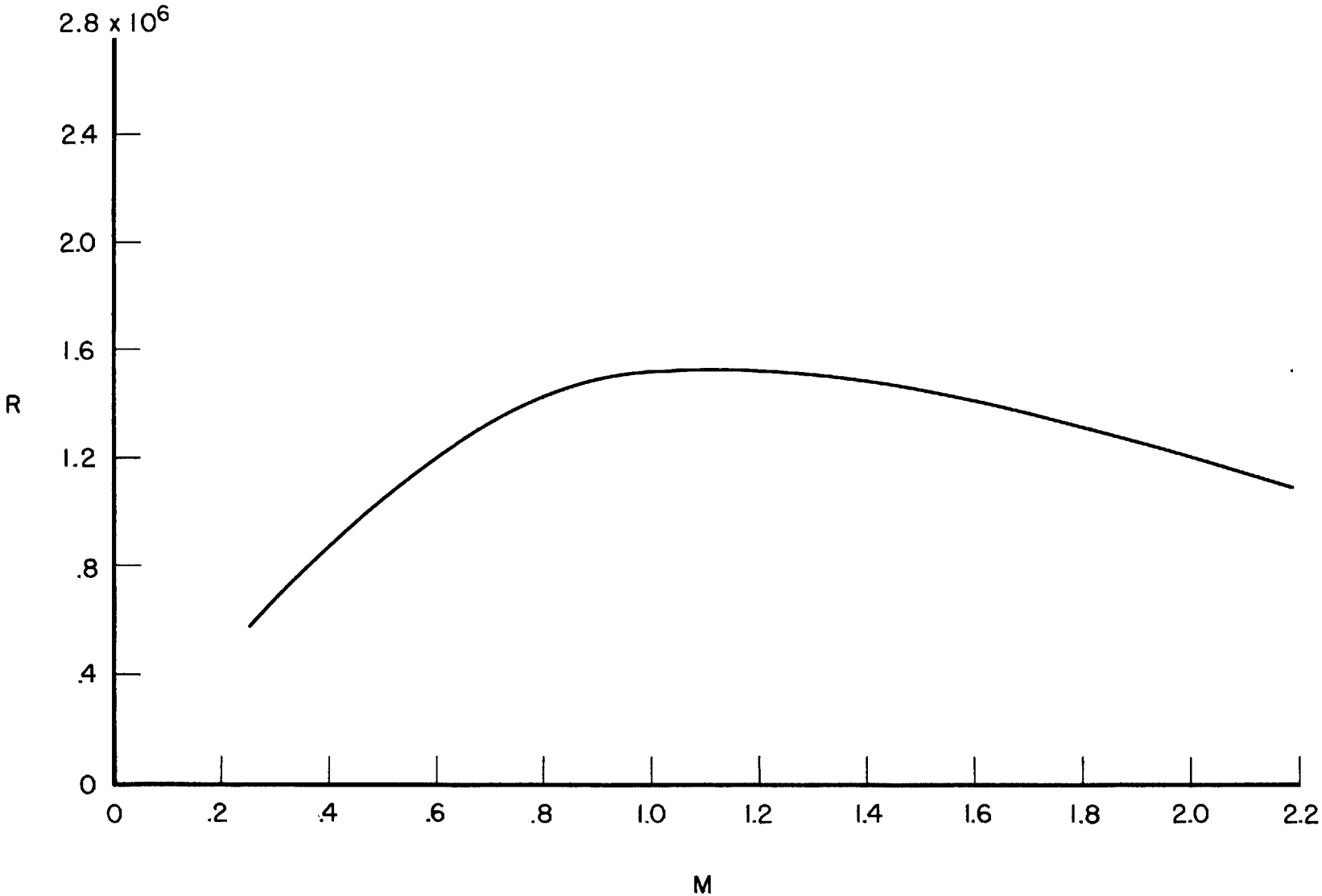

Figure 3.- Variation of Reynolds number with Mach number.

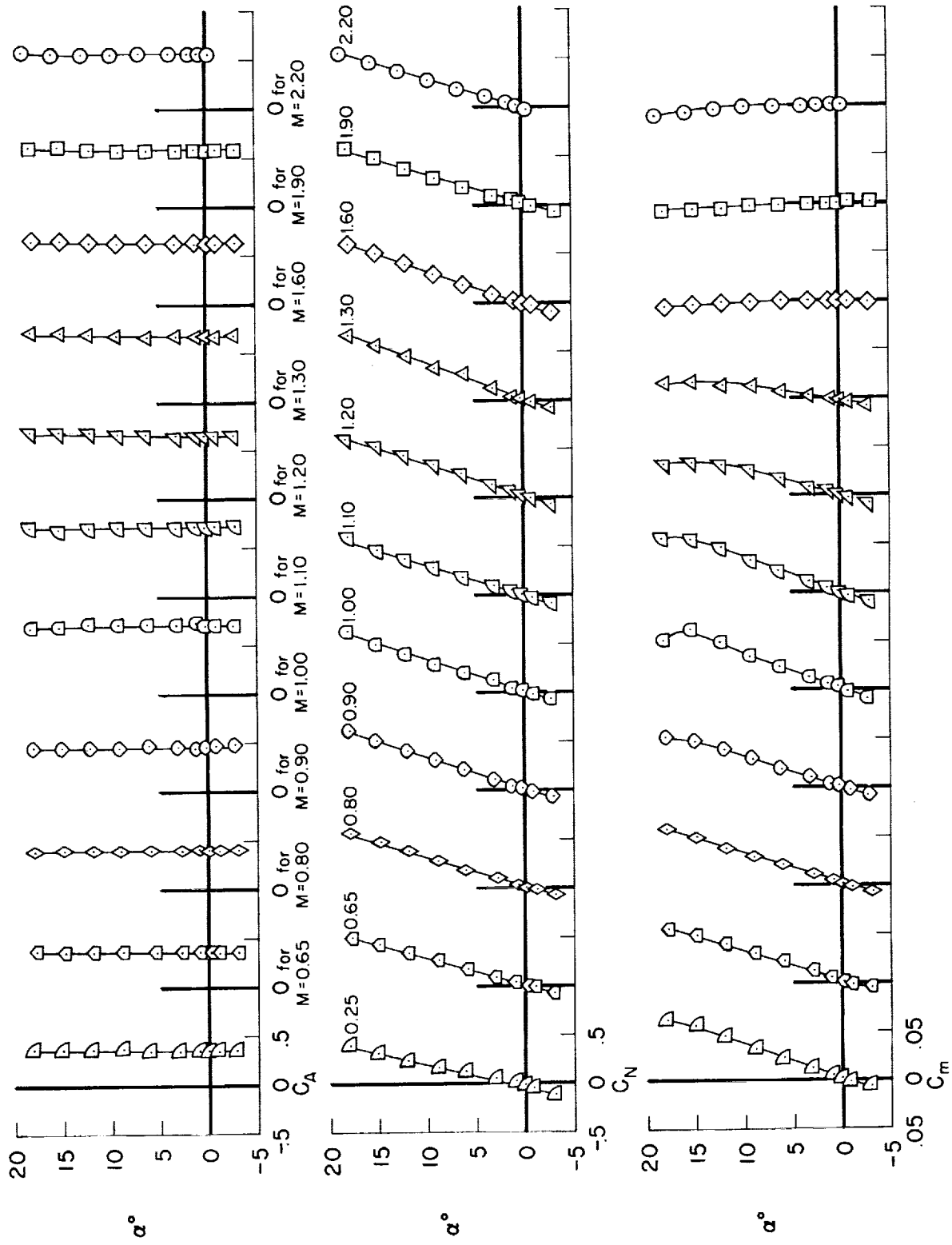

Figure 4.- Variation of static characteristics with angle of attack; basic configuration.

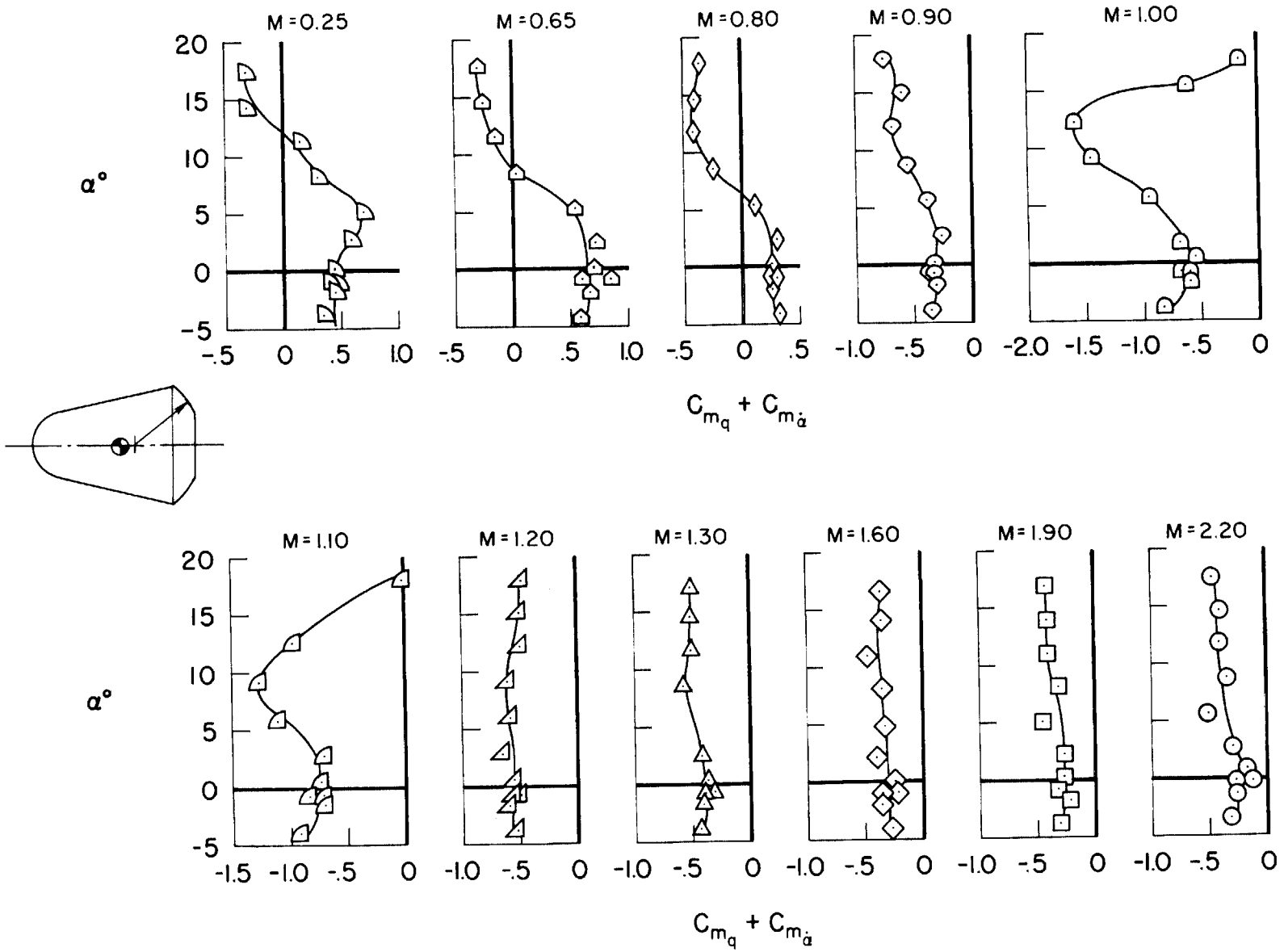

(a) Basic configuration (short radius).

Figure 5.- Variation of damping in pitch with angle of attack.

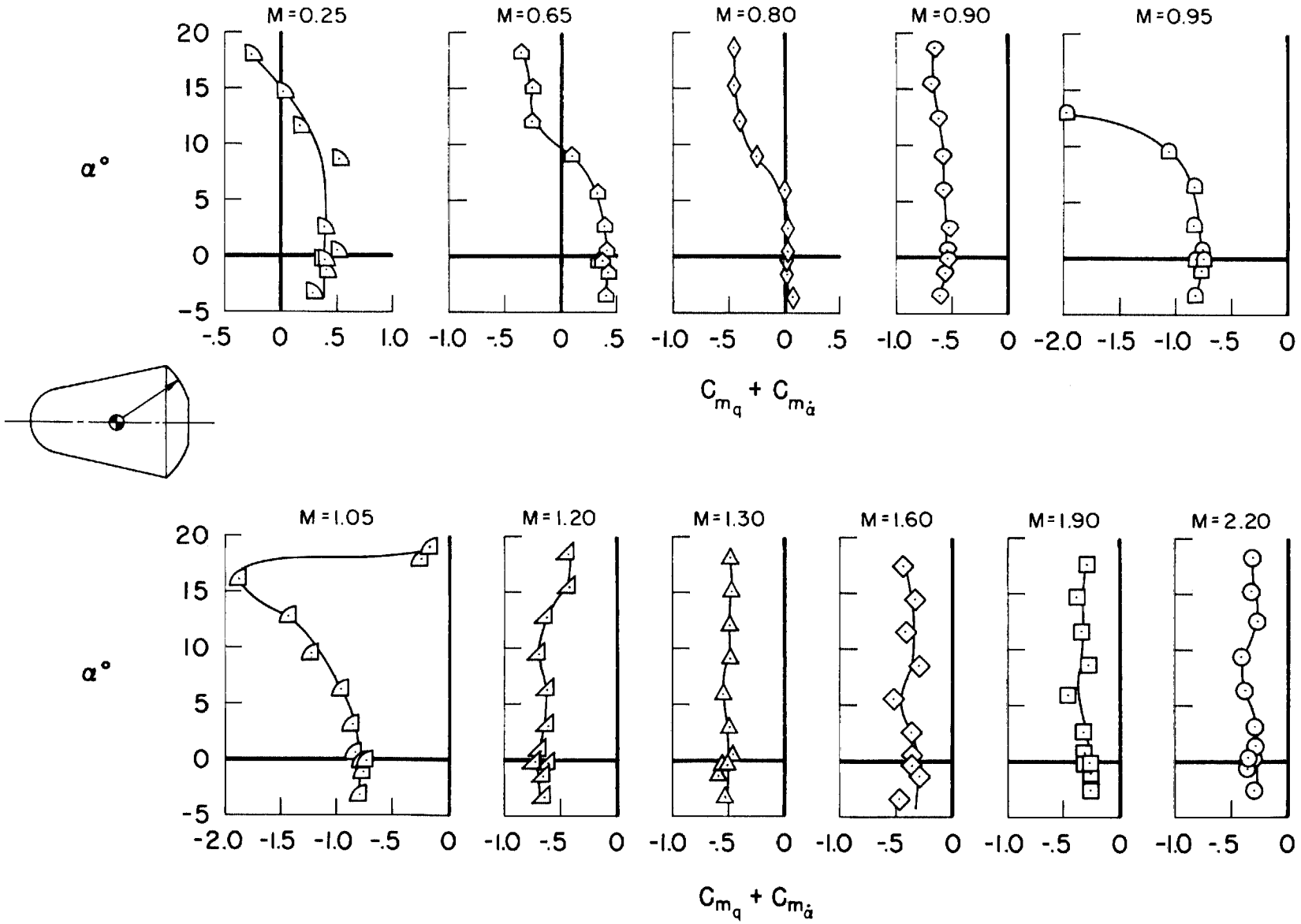

(b) Medium radius.

Figure 5.- Continued.

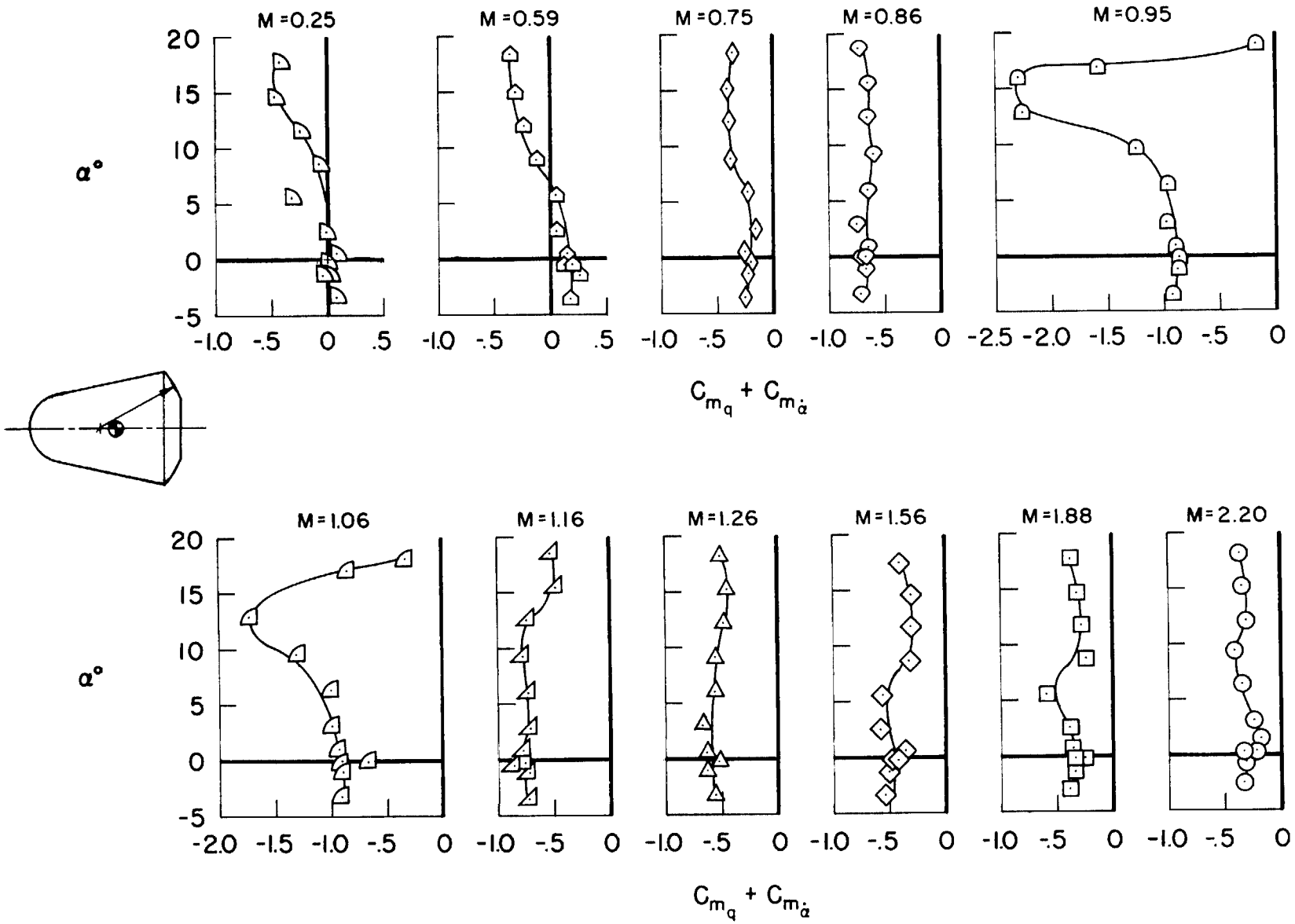

(c) Long radius.

Figure 5.- Continued.

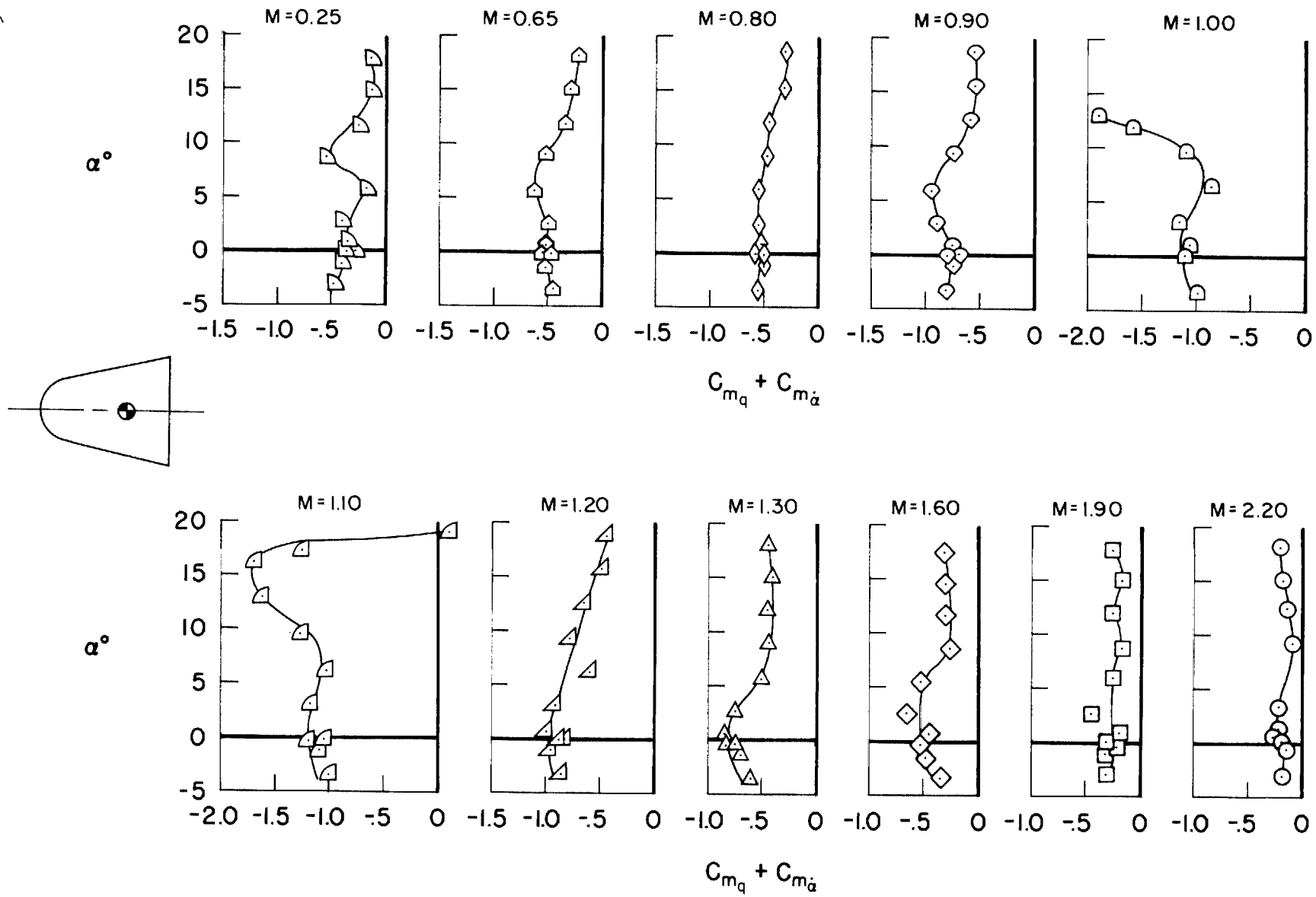

(d) Flat base.

Figure 5.- Continued.

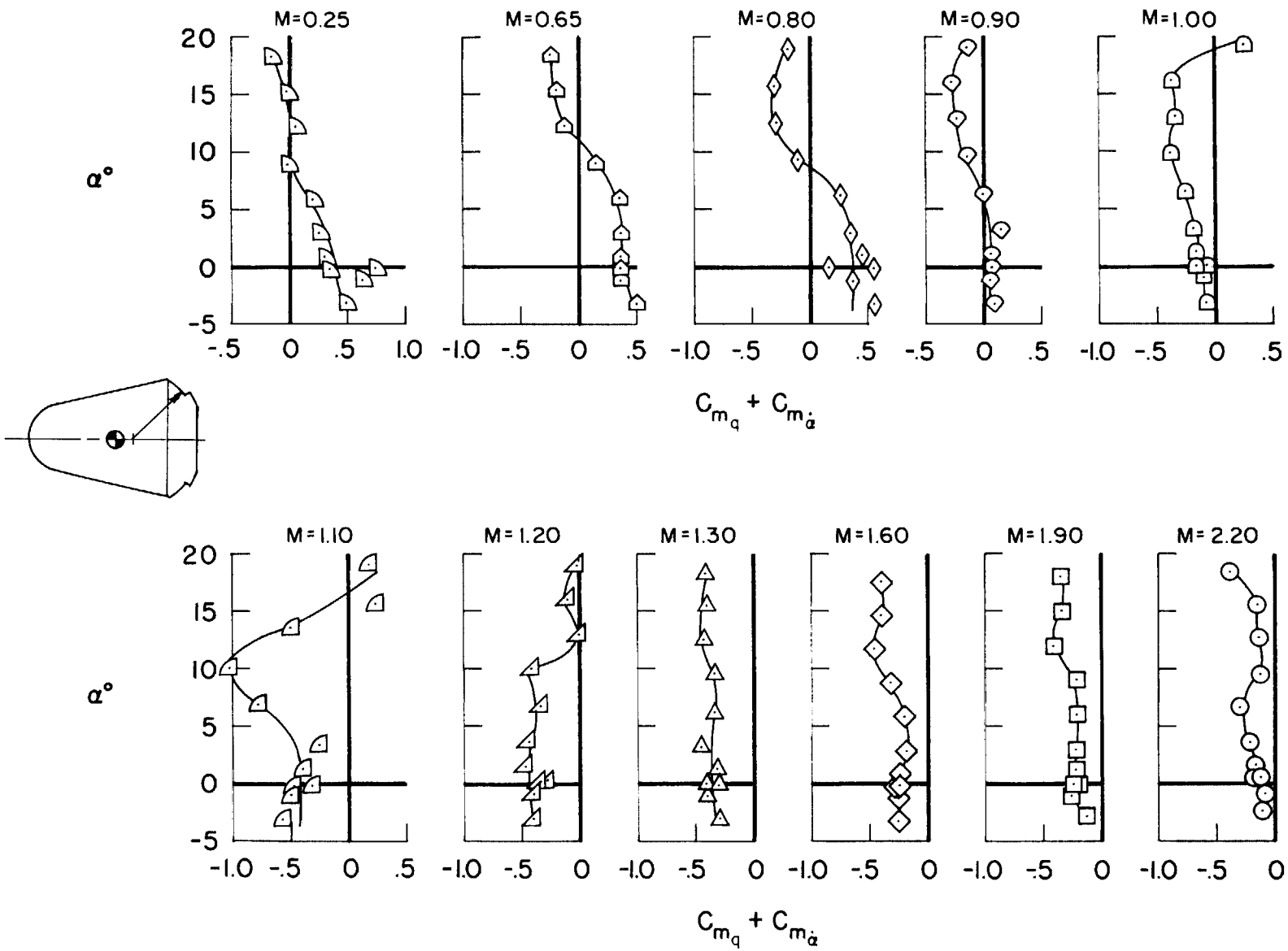

(e) Step out base.

Figure 5.- Continued.

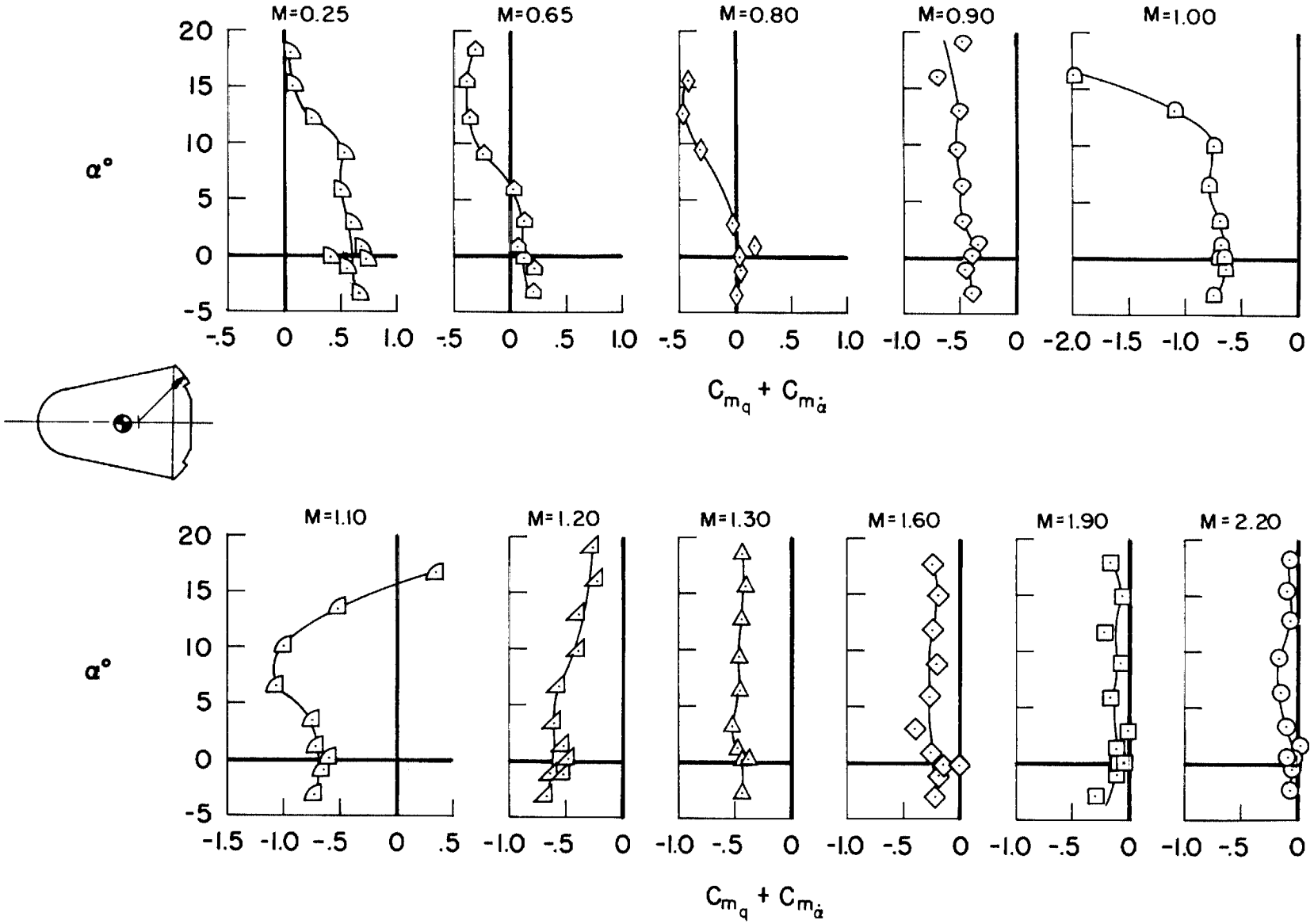

(f) Step in base.

Figure 5.- Continued.

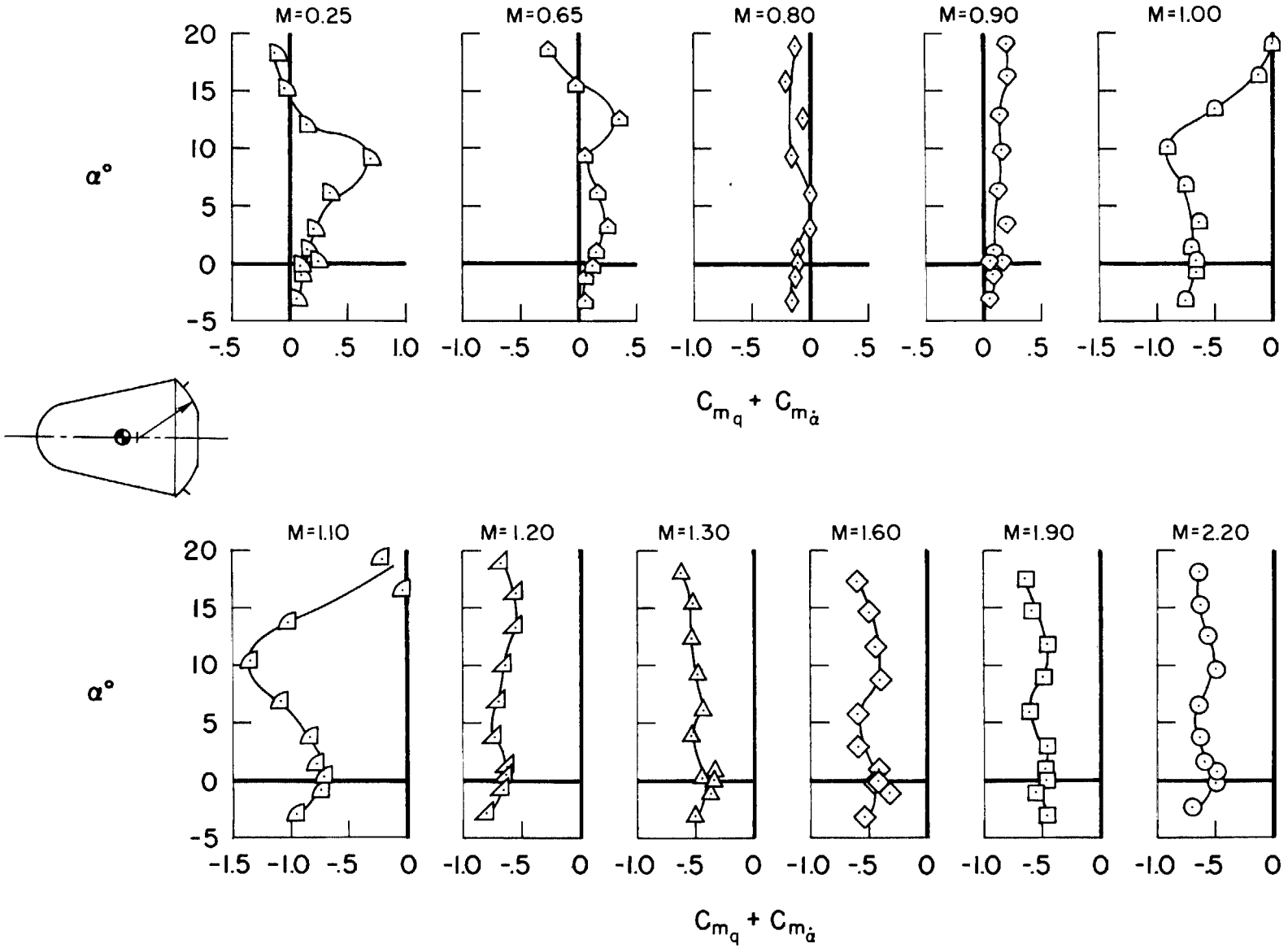

(g) Outer fence.

Figure 5.- Continued.

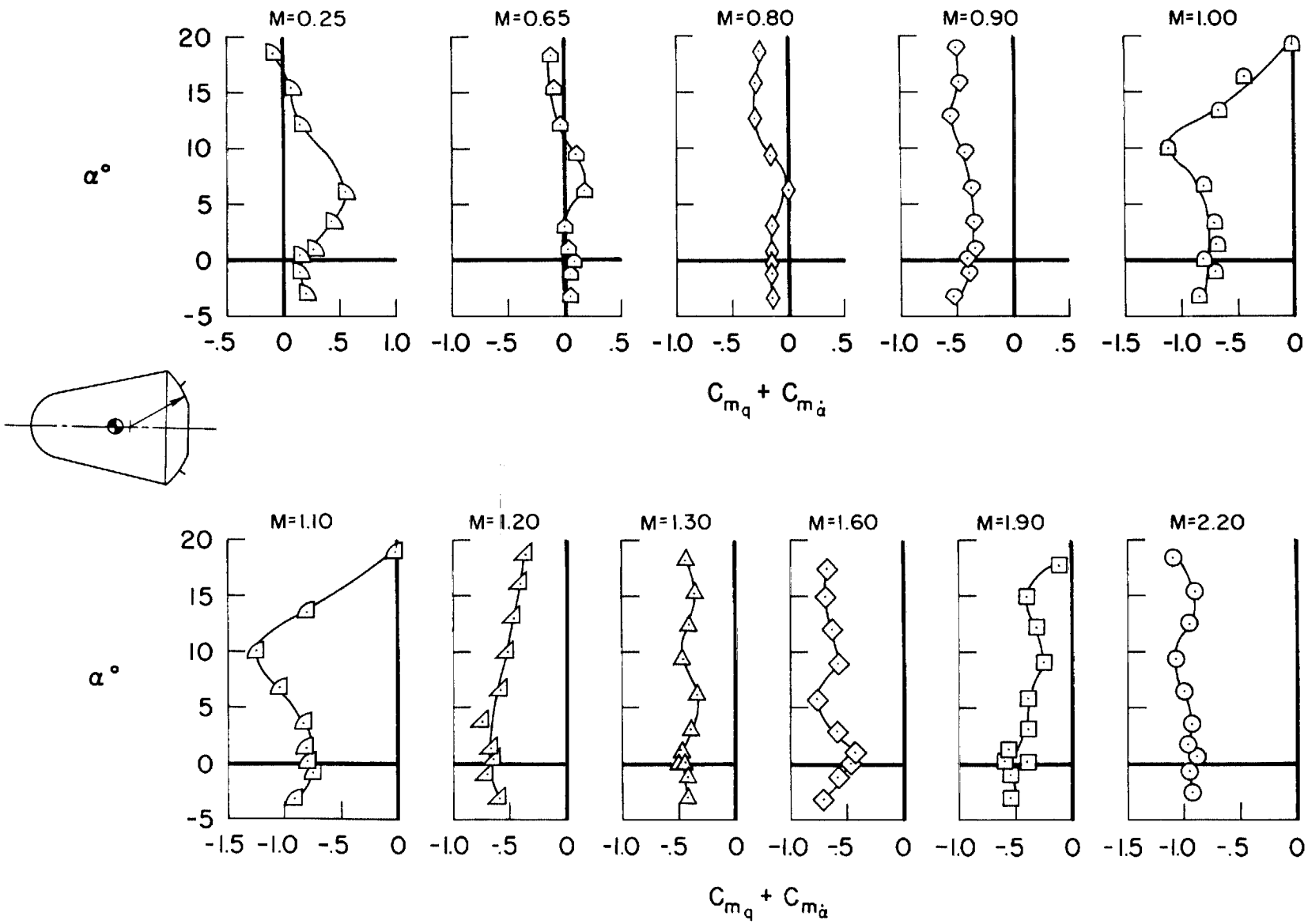

(h) Inner fence.

Figure 5.- Concluded.

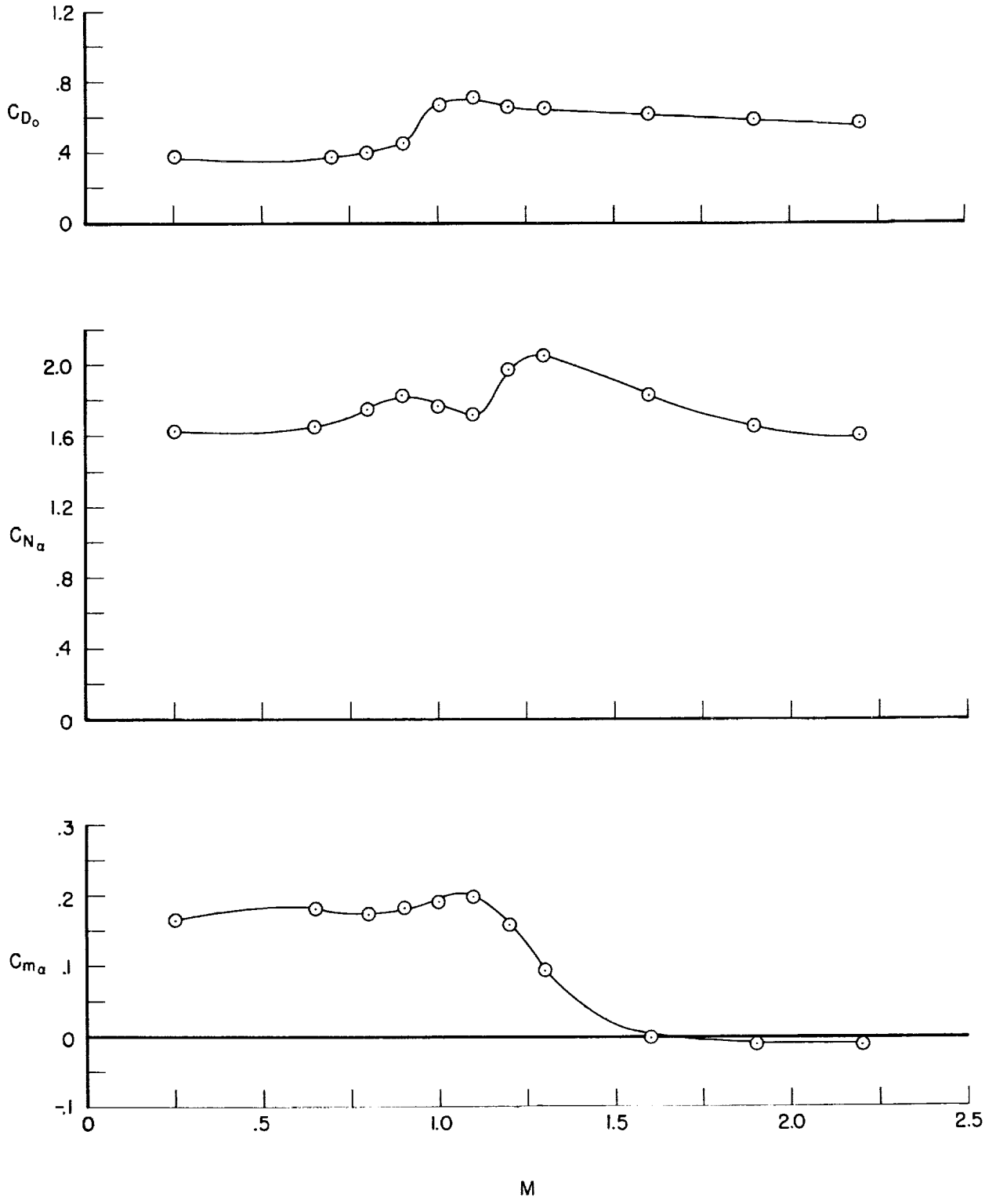

Figure 6.- Variation of static stability derivatives with Mach number; basic configuration, $\alpha = 0^{\circ}$.

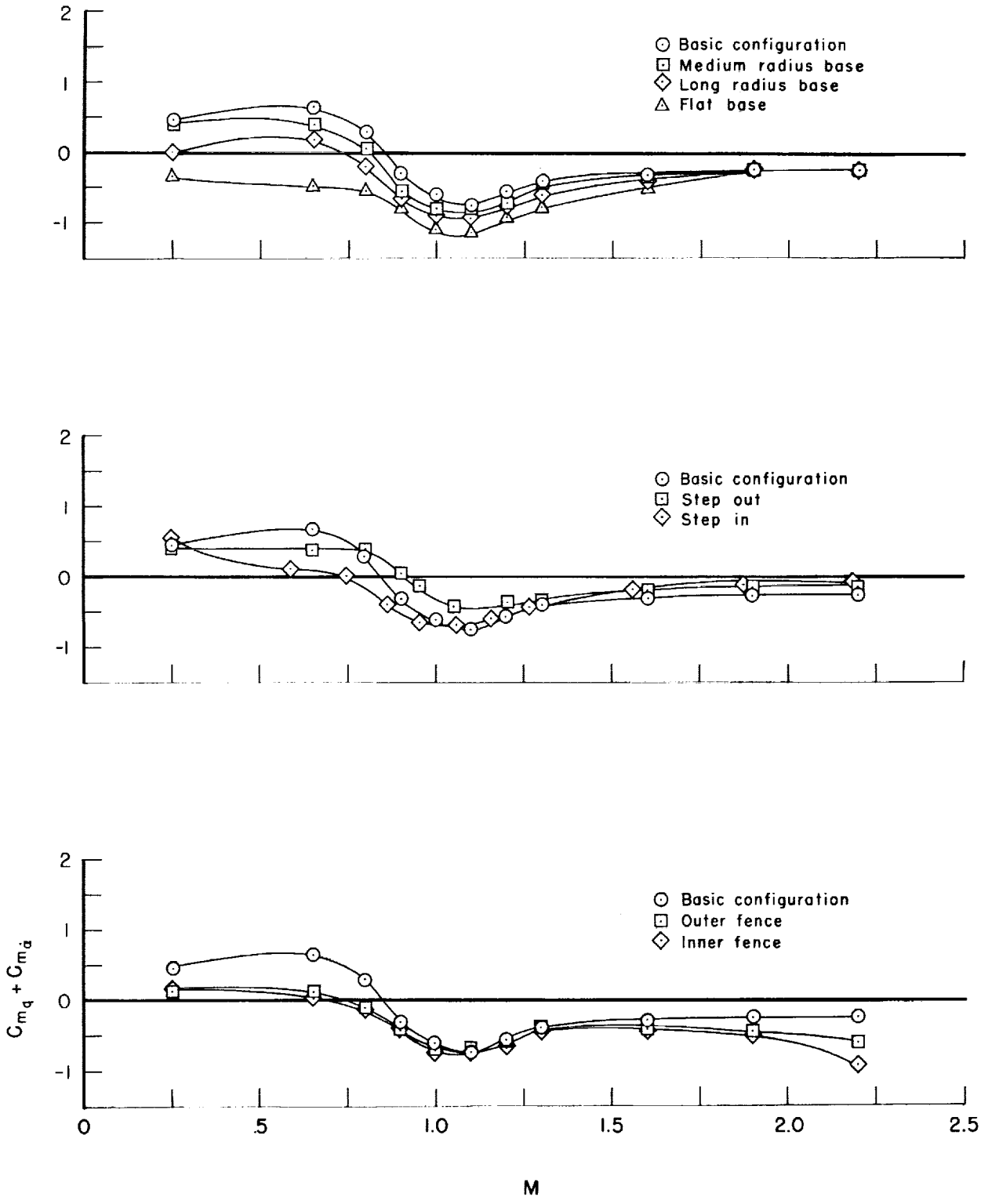

Figure 7.- Variation of damping in pitch with Mach number; $\alpha = 0^{\circ}$.

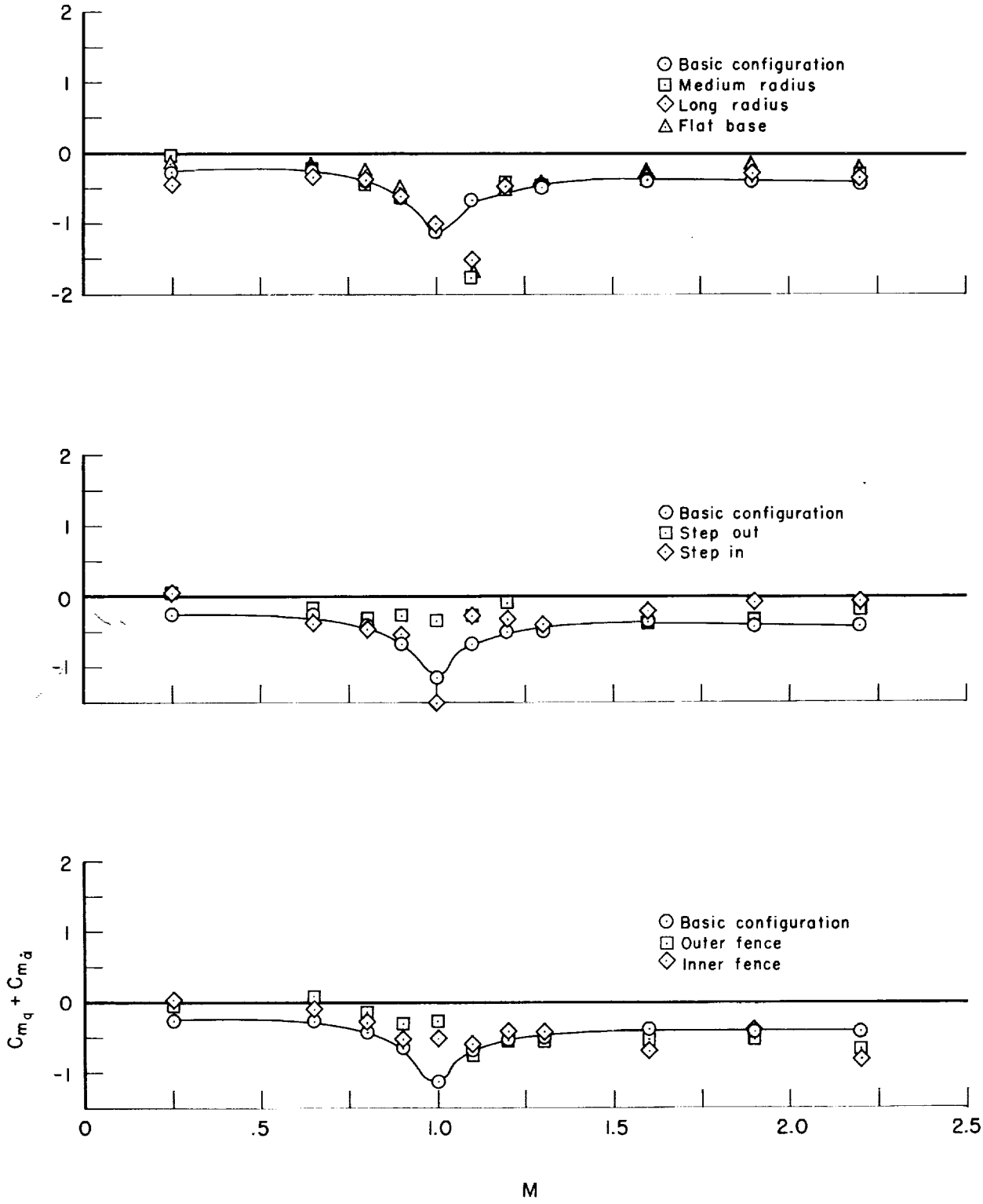

Figure 8.- Variation of damping in pitch with Mach number; $\alpha = 15^{\circ}$.